

Suppression of $1/f^\alpha$ noise in one-qubit systems

Pekko Kuopanportti,^{1,*} Mikko Möttönen,^{1,2} Ville Bergholm,¹
Olli-Pentti Saira,^{1,2} Jun Zhang,³ and K. Birgitta Whaley³

¹Laboratory of Physics, Helsinki University of Technology P. O. Box 4100, 02015 TKK, Finland

²Low Temperature Laboratory, Helsinki University of Technology, P.O. Box 3500, 02015 TKK, Finland

³Department of Chemistry and Pitzer Center for Theoretical Chemistry, University of California, Berkeley, CA 94720

(Dated: October 26, 2018)

We investigate the generation of quantum operations for one-qubit systems under classical noise with $1/f^\alpha$ power spectrum, where $2 > \alpha > 0$. We present an efficient way to approximate the noise with a discrete multi-state Markovian fluctuator. With this method, the average temporal evolution of the qubit density matrix under $1/f^\alpha$ noise can be feasibly determined from recently derived deterministic master equations. We obtain qubit operations such as quantum memory and the NOT gate to high fidelity by a gradient based optimization algorithm. For the NOT gate, the computed fidelities are qualitatively similar to those obtained earlier for random telegraph noise. In the case of quantum memory however, we observe a nonmonotonic dependency of the fidelity on the operation time, yielding a natural access rate of the memory.

I. INTRODUCTION

In solid-state realization of qubits, material specific fluctuations typically induce the major contribution to the intrinsic noise. Much effort has been focused on the preservation of the state in a quantum memory in the presence of $1/f^\alpha$ noise since this is a ubiquitous form of noise encountered in solid-state qubit applications [1, 2, 3]. Both charge and spin qubits are susceptible to noise of this form. For Josephson junctions, both charge noise [4, 5] and critical current noise [6, 7] have been measured to have $1/f^\alpha$ power spectral densities. Similar charge fluctuations are responsible for the well-known $1/f^\alpha$ nature of low frequency noise in single electron transistors [8]. Background charge fluctuations resulting in $1/f^\alpha$ noise spectra are considered to be the most important source of dephasing in Josephson junction qubits [4, 5, 9]. Spin qubits such as those formed from donor spins in semiconductors are susceptible to nuclear spin noise deriving from dipolar coupling between environmental nuclear spins. The nuclear spin bath couples to the donor spins by hyperfine interactions, which renders the dynamics of the nuclear spins to cause dephasing. Recent calculations for a phosphorus donor in silicon show that the high frequency component of the nuclear spin noise is approximately described by a $1/f^\alpha$ power spectrum [10]. Electron spin qubits implanted into silicon [11] are also affected by relaxation of dangling bonds deriving from oxygen vacancies at the Si/SiO₂ interface. This gives rise to a magnetic noise with a $1/f^\alpha$ spectrum that is the dominant mechanism for phase fluctuations of donor spins near the surface [12]. Another form of noise closely related to $1/f^\alpha$ noise is random telegraph noise (RTN), which arises from coupling of individual bistable fluctu-

ators to a qubit [2, 13, 14, 15, 16, 17, 18, 19].

Several approaches to suppress decoherence based on pulse design have been proposed in the literature. Among them, dynamical decoupling schemes average out the unwanted effects of the environmental interaction through the application of suitable control pulses [20, 21]. Application of these schemes often involves hard pulses with instantaneous switchings and unbounded control amplitudes, resulting in a range of validity restricted to time scales for which the pulse duration is much less than the noise correlation time [22, 23]. In Ref. [24], a direct pulse optimization method restricted to bounded control pulses was developed for implementing one-qubit operations in a noisy environment. This initial work on noise suppression addressed the example of a single qubit system under the influence of classically modeled random telegraph noise, such as might arise from a single bistable fluctuator.

In this paper, we extend the work of Ref. [24] to the physically relevant situation of $1/f^\alpha$ noise where $2 > \alpha > 0$. This kind of noise is known to result, for example, from a set of bistable fluctuators [25, 26, 27, 28], i.e., RTN sources. We investigate two ways to approximate the $1/f^\alpha$ noise for computer simulations, namely, the sum of independent RTN fluctuators and a single discrete multi-state Markovian noise source. We show that the single fluctuator provides a much more efficient way to model $1/f^\alpha$ noise than independent RTN fluctuators. Furthermore, the average temporal evolution of the density matrix under this Markovian noise can be exactly described by a set of deterministic master equations derived in Ref. [29]. Using this approach, we avoid the heavy computational task arising from the numerical evaluation of the density matrix averaged over a large number of different sample paths of the noise as computed in Ref. [24]. This framework will not only significantly accelerate the convergence of the control pulse sequence optimization, but also allows further theoretical analysis. Using these master equations, we employ gradient based optimization procedures to obtain pulse sequences that suppress $1/f^\alpha$ noise for quantum mem-

*Electronic address: pekko.kuopanportti@tkk.fi

ory and for a NOT gate. Comparisons with composite pulses designed to eliminate systematic errors and with refocusing pulses demonstrate that the numerically optimized pulse sequences yield the highest fidelities.

The remainder of this paper is organized as follows. In Sec. II, we show how to efficiently approximate the $1/f^\alpha$ noise by a multi-state Markovian fluctuator. In Sec. III, we define the fidelity of qubit operations, review the master equations describing the average evolution of the qubit density matrix in the presence of the noise and describe the numerical optimization procedure. Sections IV and V present optimized control pulse sequences and the achieved fidelities for quantum memory and for the NOT gate, respectively. Finally, Sec. VI concludes and indicates further applications of the method.

II. ONE-QUBIT SYSTEM SUBJECT TO $1/f^\alpha$ NOISE

We consider a one-qubit system described by the effective Hamiltonian

$$H = \frac{1}{2}a(t)\sigma_x + \frac{1}{2}\eta(t)\sigma_z, \quad (1)$$

where $a(t) \in [-a_{\max}, a_{\max}]$ is the external control field applied along the x direction and $\eta(t)$ is the classical noise signal perturbing the system along the z direction. The noise source $\eta(t)$ can be characterized by its autocorrelation function

$$C(t) \equiv \langle \eta(0)\eta(t) \rangle = \lim_{T \rightarrow \infty} \frac{1}{T} \int_{-T/2}^{T/2} \eta(s)\eta(s+t) ds, \quad (2)$$

the Fourier transformation of which defines the noise power spectral density as

$$S(f) = \int_{-\infty}^{\infty} C(t)e^{-i2\pi ft} dt. \quad (3)$$

For a single RTN source with the amplitude Δ and correlation time τ_c , the autocorrelation function is given by [30]

$$C_{\text{RTN}}(t) = \Delta^2 e^{-2|t|/\tau_c}, \quad (4)$$

and the corresponding power spectral density by

$$S_{\text{RTN}}(f) = \frac{\Delta^2 \tau_c}{1 + (\pi f \tau_c)^2}. \quad (5)$$

A standard way to simulate $1/f^\alpha$ noise is to use an ensemble of K independent uncorrelated RTN processes [1, 25, 27]. Let $\eta_k(t)$ be a symmetric RTN signal switching between values $-\Delta_k$ and Δ_k with the correlation time $\tau_k \equiv 1/\gamma_k$, where γ_k is the transition rate between the two states. The total noise process appears in the Hamiltonian (1) as $\eta(t) = \sum_{k=1}^K \eta_k(t)$. Since the

RTN sources are independent, Eqs. (2) and (4) yield the autocorrelation function

$$C(t) = \sum_{k=1}^K \Delta_k^2 e^{-2|t|/\tau_k} = \sum_{k=1}^K \Delta_k^2 e^{-2\gamma_k|t|}, \quad (6)$$

and the corresponding power spectral density is given by

$$S(f) = \sum_{k=1}^K \frac{\Delta_k^2 \gamma_k}{\gamma_k^2 + (\pi f)^2}. \quad (7)$$

Introducing the density of transition rates $g(\gamma)$ and expressing the noise strength Δ as a function of the transition rate, we can replace the summation in Eq. (7) by an integration, which yields

$$S(f) = \int_{\gamma_{\min}}^{\gamma_{\max}} \frac{\Delta^2(\gamma)g(\gamma)\gamma}{\gamma^2 + (\pi f)^2} d\gamma, \quad (8)$$

where γ_{\min} and γ_{\max} are minimal and maximal transition rates, respectively. Provided that

$$\Delta^2(\gamma)g(\gamma) = 2A/\gamma, \quad (9)$$

where A is a constant, the power spectral density in Eq. (8) becomes [27]

$$\begin{aligned} S(f) &= \frac{2A}{\pi f} \left[\arctan\left(\frac{\gamma_{\max}}{\pi f}\right) - \arctan\left(\frac{\gamma_{\min}}{\pi f}\right) \right] \\ &\simeq \frac{A}{f}, \quad \gamma_{\min} \ll \pi f \ll \gamma_{\max}. \end{aligned} \quad (10)$$

Thus Eq. (10) yields an approximation to the $1/f$ power spectrum. To generate a general $1/f^\alpha$ power spectral density for $2 > \alpha > 0$, we can choose

$$\Delta^2(\gamma)g(\gamma) = 2A\gamma^{-\alpha} \quad (11)$$

as shown in [27].

Although the above method yields a valid approximation for the $1/f^\alpha$ spectrum, it is computationally inefficient. In particular, the number of distinct noise states increases exponentially with the number of RTN fluctuators K , i.e., the number of terms in the sum of Eq. (7) approximating the $1/f^\alpha$ noise. Since the size of the differential equation system describing the average qubit dynamics increases linearly with the number of noise states [29], in practice one has to restrict the computation to a rather small number of independent RTN fluctuators.

To overcome this problem, we present a conceptually different way of generating the desired $1/f^\alpha$ noise spectrum using a single multi-state Markovian fluctuator. Consider a continuous-time Markovian noise process with M discrete noise states. Let Γ_{kj} denote the transition rate from the j th state to the k th one. In order to preserve total probability, we must have

$$\sum_{j=1}^M \Gamma_{jk} = 0 \quad \text{for all } k = 1, 2, \dots, M. \quad (12)$$

Let us assume that the transition rates are symmetric, i.e., $\Gamma = \Gamma^T$. Under this assumption the noise process has a steady-state solution in which the different noise states are equally probable. In order for the noise to be unbiased, i.e., $\langle \eta \rangle = 0$, the amplitudes b_k associated with the noise states must satisfy

$$\sum_{k=1}^M b_k = 0. \quad (13)$$

Thus the autocorrelation is given by

$$C(t) = \langle \eta(t)\eta(0) \rangle = \frac{1}{M} b^T e^{\Gamma|t|} b. \quad (14)$$

Since Γ is symmetric, we can diagonalize it with an orthogonal matrix V as $\Gamma = V\Lambda V^T$, where the real diagonal matrix $\Lambda = \text{diag}\{\lambda_k\}_{k=1}^M$ carries the eigenvalues of Γ in a descending order. Defining $\chi := \frac{1}{\sqrt{M}} V^T b$, we rewrite Eq. (14) in the form of Eq. (6) as

$$C(t) = \chi^T e^{\Lambda|t|} \chi = \sum_{k=1}^M \chi_k^2 e^{\lambda_k|t|}. \quad (15)$$

In order to use this multi-state Markovian fluctuator to approximate $1/f^\alpha$ noise, we have to choose the eigenvalues λ_k and the amplitudes χ_k such that Eq. (11) is fulfilled. Moreover, we must construct the orthogonal matrix V such that $\Gamma = V\Lambda V^T$ satisfies Eq. (12), the amplitudes b_k satisfy Eq. (13), and the off-diagonal elements of Γ must be non-negative.

One way to satisfy these requirements is to pick an integer $m \geq 2$ and set $M = 2^m$ and to choose the eigenvalues as

$$\{\lambda_k\}_{k=1}^M = -2\{0, \gamma_{\min}, \gamma_{\min} + \delta, \gamma_{\min} + 2\delta, \dots, \gamma_{\max}\},$$

where $\gamma_{\max} = (M-2)\delta + \gamma_{\min}$ and $0 < \delta \leq \gamma_{\min}$. Hence, the distribution of the transition rates $g(\gamma)$ is uniform on $[\gamma_{\min}, \gamma_{\max}]$. Then we set $V = H^{\otimes m}$, where H is the Hadamard matrix

$$H = \frac{1}{\sqrt{2}} \begin{pmatrix} 1 & 1 \\ 1 & -1 \end{pmatrix}.$$

Explicit calculation shows that these choices ensure that Eq. (12) is satisfied. To fulfill Eqs. (11) and (13), we set $\chi_1 = 0$ and $\chi_k = \gamma_k^{-\alpha/2}$ for $k = 2, \dots, M$, where γ_k is equal to $\gamma_{\min} + (k-2)\delta$. It can be shown that this construction will also produce transition matrices Γ with non-negative off-diagonal elements. Hence we have provided an efficient way to implement $1/f^\alpha$ noise. Note that the M -state Markovian fluctuator, Eq. (15), corresponds formally to Eq. (6) with $M-1$ non-vanishing RTN fluctuators. Thus we have achieved an exponential improvement in the efficiency of the noise approximation. Alternatively, we can choose the eigenvalues of Γ freely and obtain a valid matrix V with numerical optimization,

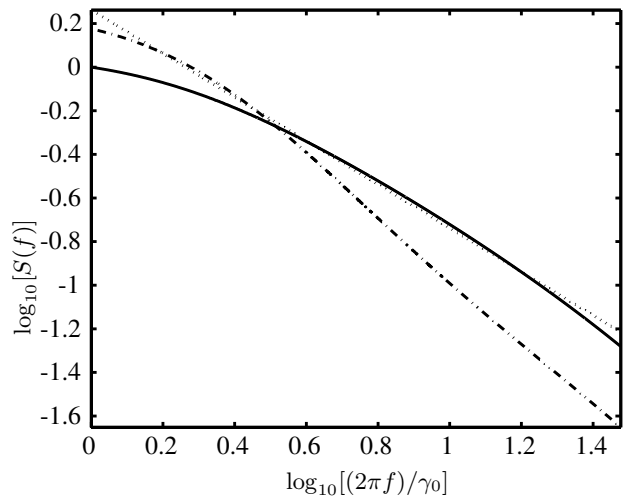


FIG. 1: Logarithm of the power spectral density for five independent RTN fluctuators (dash-dotted line), a multi-state Markovian source corresponding to 31 RTN fluctuators (solid line), and an ideal $1/f$ noise (dotted line). The transition rates of the RTN fluctuators are in both cases distributed uniformly on the interval $[\gamma_0, 30\gamma_0]$.

which may result in even more faithful approximation of $1/f^\alpha$ noise.

Figure 1 compares the approximation of the spectral density of $1/f$ noise generated by independent RTN sources and by a multi-state Markovian source. For the RTN approach, we choose 5 independent noise sources, for which the transition rates γ_k are uniformly distributed in the range $[\gamma_{\min}, \gamma_{\max}] = [\gamma_0, 30\gamma_0]$, and the strengths are given by $\Delta_k = 1/\sqrt{\gamma_k}$. This yields a fluctuator with 32 distinct noise states. For the multi-state fluctuator, we choose a 32-state noise source, for which the nonzero eigenvalues λ_k of its transition rate matrix Γ are distributed uniformly on $[-60\gamma_0, -2\gamma_0]$, and $\chi_k = 1/\sqrt{-\lambda_k/2}$. Thus the condition in Eq. (9) is satisfied for both of the approaches and the multi-state noise source has an autocorrelation function and power spectral density which are equal to those for a certain ensemble of 31 RTN fluctuators. We employ representations of similar computational complexity here in order to be able to assess the relative accuracy for a given computational effort.

Figure 1 shows that an ensemble of five RTN processes is not an accurate model for $1/f$ noise, whereas a single 32-state Markovian noise source is quite accurate, especially in the range $3\gamma_0 \lesssim \omega \lesssim 16\gamma_0$. The poor quality of the approximation with five RTN fluctuators is due to the small number of independent noise sources employed here, whereas the 32-state Markovian fluctuator contains more parameters and thereby introduces more flexibility in the noise approximation. The frequency range over which the approximation is accurate is relatively short if one considers that the $1/f$ noise detected in experimental applications often extends over several frequency decades. The width of this frequency range can of course be increased by increasing the width of the region from which the eigenvalues of the matrix Γ are chosen. In

this case, however, the number of discrete levels in the Markovian source must also be increased to preserve the desired accuracy. For the main purpose of demonstrating the feasibility of the numerical optimization algorithm, in the rest of this paper we will continue to approximate $1/f^\alpha$ noise by a single Markovian noise source with 32 levels.

III. QUBIT DYNAMICS AND CONTROL

In Ref. [24], the temporal evolution of the qubit density matrix was calculated by averaging over 10^4 – 10^5 unitary quantum trajectories, each corresponding to a sample noise path. To ensure accuracy, a large number of unitary trajectories are required, which results in extensive computational effort. In Ref. [29], exact deterministic master equations describing the average temporal evolution of quantum systems under Markovian noise were derived.

Following Ref. [29], we introduce a conditional density operator $\rho_k(t)$ which corresponds to the density operator of the system averaged over all the noise sample paths occupying the k th state at the time instant t . The conditional density operators are normalized such that the trace of the operator $\rho_k(t)$ yields the probability of the k th noise state as $P_k(t) = \text{Tr}[\rho_k(t)]$. The total average density operator can be expressed as

$$\rho(t) = \sum_k \rho_k(t). \quad (16)$$

The dynamics of ρ_k is obtained from the coupled master equations [29]

$$\partial_t \rho_k(t) = \frac{1}{i\hbar} [H_k(t), \rho_k(t)] + \sum_j \Gamma_{kj} \rho_j(t), \quad (17)$$

where $H_k(t)$ is the Hamiltonian of the system corresponding to the k th noise state, and Γ_{kj} the transition rate from the j th state to the k th state, as defined in Sec. II. Specifically, in our one-qubit case,

$$H_k(t) = \frac{1}{2}a(t)\sigma_x + \frac{1}{2}b_k\sigma_z, \quad (18)$$

where b_k is the noise amplitude of the state k . We shall use $\mathcal{E}_a\{\rho\}$ to denote the state ρ evolved under the influence of noise and the control sequence a .

The fidelity function quantifying the overlap between the desired state ρ_f and the actual achieved final state is defined as

$$\phi(\rho_f, \mathcal{E}_a\{\rho_0\}) = \text{Tr}[\rho_f^\dagger \mathcal{E}_a\{\rho_0\}], \quad (19)$$

where ρ_0 is the initial state of the system. To measure how close the evolution \mathcal{E}_a is to the intended quantum gate operation U , we calculate the average of the fidelity

$\phi(U\rho_0U^\dagger, \mathcal{E}_a\{\rho_0\})$ over all pure initial states ρ_0 , and obtain the gate fidelity function [24]

$$\Phi(U) = \frac{1}{2} + \frac{1}{12} \sum_{k=x,y,z} \text{Tr}[U\sigma_kU^\dagger \mathcal{E}_a\{\sigma_k\}]. \quad (20)$$

We aim to find the optimal control pulses which maximize the fidelity of the achieved quantum operation, and hence apply a typical gradient based optimization algorithm such as the gradient ascent pulse engineering (GRAPE) method developed in Ref. [31]. If the continuous pulse profiles are approximated by piecewise constant functions, the gradient of the fidelity function with respect to these constant pulse values and durations can be calculated by the chain rule. This gradient is further used as a proportional adjustment to update the control pulse profile. The optimization procedure is terminated when certain desired accuracy is achieved. Note that due to the non-convex nature of the problem, the gradient based algorithm will only yield a locally optimal solution. We further employ a multitude of initial conditions to find a control pulse which achieves the highest fidelity.

IV. QUANTUM MEMORY

In this section, we focus on the implementation of quantum memory, i.e., the identity operator. For the purpose of comparison with the optimized pulse sequences, we introduce four other kinds of control schemes which generate the identity operator.

The first reference sequence is simply not to apply any external control pulse, i.e., $a(t) = 0$. This pulse has no compensation for decoherence or error. The second reference sequence is a constant 2π pulse given by

$$a_{2\pi}(t) = a_{\max}, \quad \text{for } t \in [0, 2\pi\hbar/a_{\max}]. \quad (21)$$

The third reference sequence is the composite pulse sequence known as compensation for off-resonance with a pulse sequence (CORPSE), which was originally designed to correct systematic errors in the implementation of one-qubit quantum operations and to provide high order control protocols for systematic qubit bias, i.e., for the noise correlation time $\tau_c \rightarrow \infty$ [32, 33]. For the identity operation, the CORPSE pulse sequence can be obtained as

$$a_{\text{SC}2\pi}(t) = \begin{cases} a_{\max}, & \text{for } 0 < t' < \pi \\ -a_{\max}, & \text{for } \pi \leq t' \leq 3\pi \\ a_{\max}, & \text{for } 3\pi < t' < 4\pi, \end{cases} \quad (22)$$

where the dimensionless time t' is defined as $t' = a_{\max}t/\hbar$.

In the absence of noise, the CORPSE sequence generates the identity operator exactly although it requires twice as long operation time as a 2π pulse, the second reference pulse above. In the presence of small systematic errors, the CORPSE sequence is much more accurate

than the 2π pulse. For example, consider a state transformation from the north pole back to itself on the Bloch sphere. For $\eta(t) \equiv \Delta$ in Eq. (1), the fidelities defined in Eq. (19) can be derived to be

$$\phi_{2\pi} = 1 - \frac{\pi^2}{4} \left(\frac{\Delta}{a_{\max}} \right)^4 + O \left(\frac{\Delta}{a_{\max}} \right)^6, \quad (23)$$

and

$$\phi_{\text{SC}2\pi} = 1 - 4\pi^2 \left(\frac{\Delta}{a_{\max}} \right)^8 + O \left(\frac{\Delta}{a_{\max}} \right)^{10}. \quad (24)$$

We observe that the error in the fidelity of the 2π pulse is fourth order in the relative noise strength Δ/a_{\max} , whereas for the CORPSE pulse sequence it is eighth order. Thus the CORPSE sequence is much more accurate than a 2π pulse in correcting the effects of systematic errors on quantum memory.

The fourth standard pulse sequence which we take as a reference is the Carr-Purcell-Meiboom-Gill (CPMG) [34] sequence which is designed to preserve qubit coherence. In our context, this sequence consists of a $\pi/2$ pulse followed by multiple π pulses at intervals t_p , followed by a final $\pi/2$ pulse to bring the system back to the original state. This pulse sequence is designed for T_2 measurements on spins, starting from the $|0\rangle$ state. Thus one does not expect a CPMG pulse sequence to perform as well if the initial state is averaged over the Bloch sphere as is done to compute a gate fidelity.

We first present the fidelities obtained for the identity operator using the various control pulse options in the presence of $1/f$ noise. The noise is generated here by the single Markovian noise source discussed in Sec. II, with transition rates distributed uniformly over the interval $[1/\tau_c, 30/\tau_c]$. In Fig. 2, the fidelities obtained from optimized control pulses, 2π pulse, CORPSE, CPMG, and zero pulse sequences are plotted as functions of the characteristic correlation time τ_c of the approximate $1/f$ noise. Here, CPMG1 and CPMG2 refer to two CPMG types of pulses with the intervals between π pulses being π and 2π , respectively. The total duration for these pulses are all $12\pi\hbar/a_{\max}$. The optimal control pulse is designed for 6π , and therefore we repeat it twice. Similarly, we repeat the 2π pulse 6 times, the CORPSE sequence 3 times, the CPMG1 sequence 3 times, and the CPMG2 sequence twice. The optimal control pulse yields clearly the highest fidelity among all these pulses, whereas the zero pulse sequence has the worst performance as there are no correction mechanisms. Note that due to motional narrowing, all curves approach unit fidelity in the limit $\tau_c \rightarrow 0$.

The memory access rate is an important specification in modern computer technology [35]. In our context, it corresponds to the total duration of the control pulses. Figure 3 shows the fidelity as a function of the duration for the numerically optimized control pulses. Equation (1) implies that in the absence of noise, the quantum system will generate an identity operator for $a = a_{\max}$

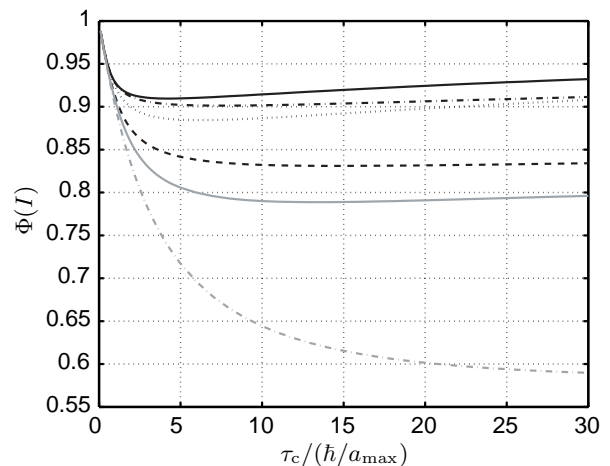


FIG. 2: Fidelity of the quantum memory as a function of the characteristic correlation time τ_c for optimized control pulses (black solid), a 2π pulse (black dash-dotted), CORPSE pulse sequence (black dotted), CPMG1 pulse sequence (black dashed), CPMG2 pulse sequence (gray solid), zero pulse sequence (gray dash-dotted). The operation time is chosen to be $12\pi\hbar/a_{\max}$. The noise is produced by a single 32-state Markovian source with the average strength $\langle|\eta|\rangle = 0.125 \times a_{\max}$ corresponding to 31 RTN fluctuators with the transition rates uniformly distributed over the region $[1/\tau_c, 30/\tau_c]$ and strengths chosen as described in Sec. II.

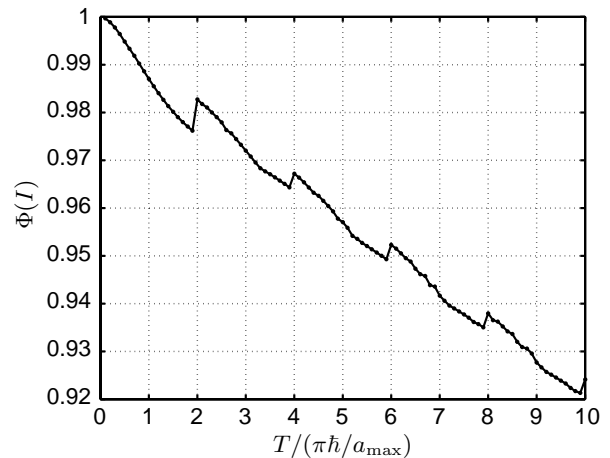


FIG. 3: Fidelity of the quantum memory as a function of the operation time for control pulses optimized at each point. The noise is produced by a similar multi-state Markovian source as in Fig. 2, with $\tau_c = 3\hbar/a_{\max}$.

and the duration $T = 2n\pi/a_{\max}$. In Fig. 3, we observe that, despite an overall decrease, there are peaks in the fidelity near these operation times. Thus we can regard $2n\pi/a_{\max}$ as the natural periods for quantum memory, and we always choose the total duration of control pulses correspondingly.

Here, we study the relation between the optimized fidelities achieved above and the average noise strength $\langle|\eta|\rangle$, for a fixed value of the characteristic correlation

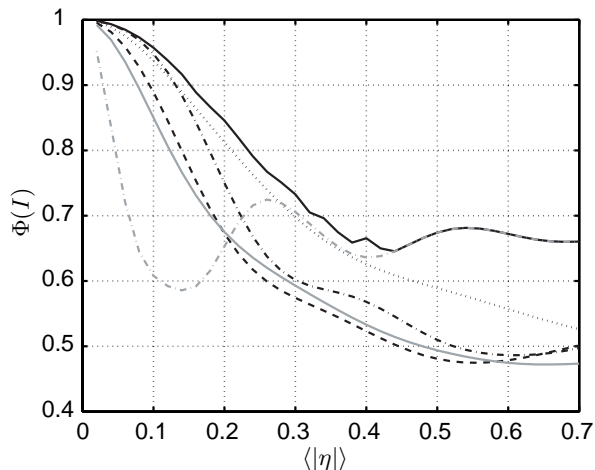


FIG. 4: Fidelity of the quantum memory as a function of the average absolute noise strength for optimized control pulses (black solid), 2π pulse (black dash-dotted), CORPSE (black dotted), CPMG1 (black dashed), CPMG2 (gray solid), and zero (gray dash-dotted). The operation time is chosen to be $12\pi\hbar/a_{\max}$. Except for its strength, the noise is produced by a similar multi-state Markovian source as in Fig. 2 with the correlation time $\tau_c = 30\hbar/a_{\max}$.

time $\tau_c = 30\hbar/a_{\max}$. Figure 4 shows the fidelity as a function of the noise strength for the optimized control pulses, 2π pulse, the CORPSE, CPMG1, CPMG2, and zero pulse sequences. At small values of $\langle|\eta|\rangle$ again, the optimized control pulses consistently achieve higher fidelities than all reference pulses. However, we note that if the noise strength exceeds ~ 0.4 , the optimized pulse sequence reduces to the zero pulse sequence, i.e., any nonzero pulse sequence will actually deteriorate the fidelity performance.

The discussion above is based on the specific noise density spectrum $1/f^\alpha$ with $\alpha = 1$. Figure 5 shows the fidelities of quantum memory for four optimized control pulses, each of which is obtained for a different value of α . The noise is produced here by a single multi-state Markovian source with average strength $\langle|\eta|\rangle = 0.125 \times a_{\max}$, and the total duration for all control pulses are fixed to 6π . A systematic scaling of the correlation time axis with respect to α is clearly visible in Fig. 5. This phenomenon is explained by the fact that the concentration of the power spectrum of $1/f^\alpha$ to high frequencies, i.e., long correlation times, increases with α . Hence, the curves scale down in τ_c with increasing α .

V. NOT GATE

In this section, we focus on the generation of high-fidelity NOT gates, i.e., the σ_x operator, under $1/f$ noise. As in the case of quantum memory, we compare the numerically optimized results with reference pulses. In this

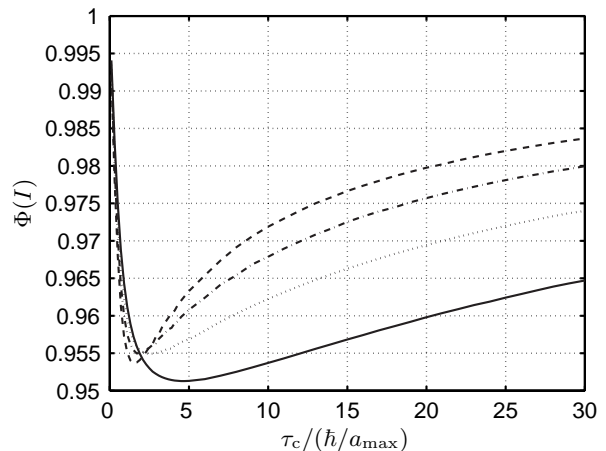


FIG. 5: Fidelity of the quantum memory achieved with optimized control pulses as a function of the characteristic correlation time τ_c for $1/f^\alpha$ noise with $\alpha = 1$ (solid), $\alpha = 1.25$ (dotted), $\alpha = 1.5$ (dash-dotted), and $\alpha = 1.75$ (dashed). The operation time is chosen to be $6\pi\hbar/a_{\max}$. The noise is produced by a similar multi-state Markovian source as in Fig. 2 with variable values of the power α .

case, our first reference pulse is the π pulse given by

$$a_\pi(t) = a_{\max}, \quad \text{for } t \in [0, \pi\hbar/a_{\max}], \quad (25)$$

which in the absence of noise is the most efficient way of achieving a NOT gate. In addition, we will use the two composite pulse sequences CORPSE and short CORPSE [32, 33] which assume here the form

$$a_{C\pi}(t) = \begin{cases} a_{\max}, & \text{for } 0 < t' < \pi/3 \\ -a_{\max}, & \text{for } \pi/3 \leq t' \leq 2\pi \\ a_{\max}, & \text{for } 2\pi < t' < 13\pi/3, \end{cases} \quad (26)$$

and

$$a_{sC\pi}(t) = \begin{cases} -a_{\max}, & \text{for } 0 < t' < \pi/3 \\ a_{\max}, & \text{for } \pi/3 \leq t' \leq 2\pi \\ -a_{\max}, & \text{for } 2\pi < t' < 7\pi/3, \end{cases} \quad (27)$$

respectively. Both of these pulse sequences correct for systematic error, CORPSE being more efficient. However, the operation time of short CORPSE is much shorter than that of CORPSE, and hence it can yield higher fidelities in the presence of noise.

Figure 6 shows the NOT gate fidelities obtained by the reference and optimized pulses in the presence of the same $1/f$ noise as employed in the analysis of quantum memory in Sec. IV. We observe that for long enough correlation times, the composite pulse sequences provide good error correction. Furthermore, as observed earlier for RTN [24], for intermediate correlation times, short CORPSE achieves the highest fidelity among the reference pulses. Figure 7 presents the pulse sequences obtained from the numerical optimizations for three different values of the noise correlation time τ_c . For the optimized pulse sequence, we find a transition from an

approximately constant pulse to a short CORPSE-like pulse sequence at characteristic correlation time $\tau_c \approx 50\hbar/a_{\max}$. This change in optimal pulse sequence is responsible for the apparent discontinuity in the first derivative of the fidelity curve in Fig. 6.

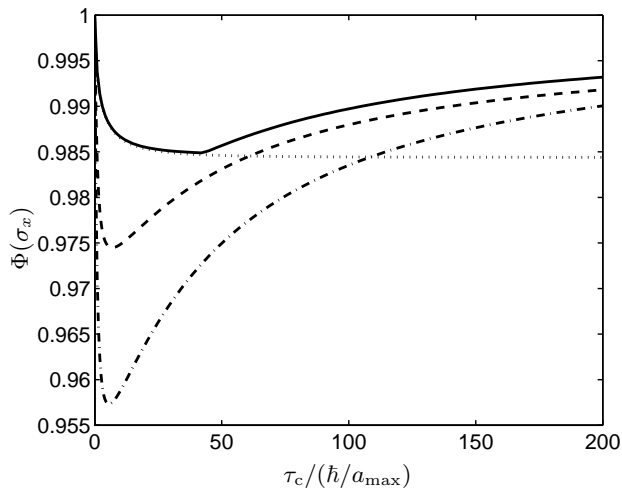


FIG. 6: NOT gate fidelities as functions of the characteristic noise correlation time τ_c for a π pulse (dotted), CORPSE (dash-dotted), short CORPSE (dashed), and gradient optimized pulse sequence (solid). The $1/f$ noise is generated as in Fig. 2.

These results for the generation of NOT gates under $1/f$ noise are qualitatively quite similar to the previous results presented in Refs. [24, 29] for a single RTN. This similarity is due to the fact that $1/f$ noise can be regarded as arising from a sum of independent RTN fluctuators, each of which having a similar fidelity dependence on their correlation times. Note that the scale for the reference correlation time τ_c of the fidelity obtained in presence of $1/f$ noise in Fig. 6 is somewhat different from the corresponding scale for the correlation time of a single RTN source, since the $1/f$ noise involves an ensemble of RTN fluctuators with a range of correlation times.

VI. CONCLUSIONS

We have studied a single qubit under the influence of $1/f^\alpha$ noise for $2 > \alpha > 0$ and investigated how decoherence due to this noise can be suppressed in the implementation of single qubit operations. We presented an efficient way to approximate the noise with a discrete multi-state Markovian fluctuator. Due to this finding, the average temporal evolution of the qubit density matrix under $1/f^\alpha$ noise can be efficiently determined from a deterministic master equation.

Employing these exact deterministic master equations describing the temporal evolution of the qubit density operator under Markovian noise, we applied a gradient

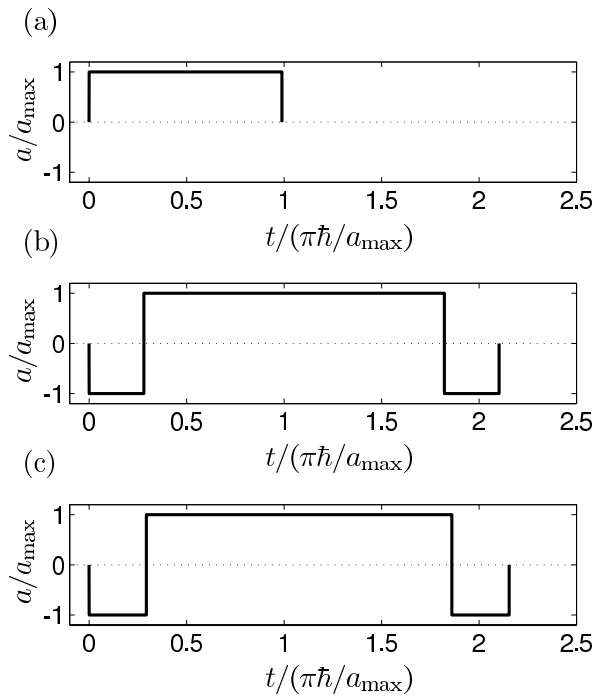


FIG. 7: Optimized pulse sequences yielding the highest gate fidelities for correlation times (a) $45\hbar/a_{\max}$, (b) $100\hbar/a_{\max}$, and (c) $150\hbar/a_{\max}$ corresponding to Fig. 6.

based optimization procedure to search for optimal control pulses implementing quantum operations. In particular, we studied the physical application of quantum memory, i.e., the identity operator, which is a fundamental concept in the realization of a quantum computer. The optimized control pulses significantly improved the fidelity over several reference sequences such as 2π , CORPSE, CPMG, and zero pulses. We observe peaks on fidelity curves corresponding to integer multiples of $2\pi\hbar/a_{\max}$ in the total durations of control pulses, where a_{\max} is the maximum magnitude of the external control field. We also studied the performance of optimal control pulses under $1/f^\alpha$ noise for several different values of $2 > \alpha \geq 1$, and found a monotonic behavior in the noise frequency as a function of α , i.e., the fidelity curves are scaled down in the correlation time for increasing α . We also investigated how the fidelities degraded as the noise strength increases. For the generation of high-fidelity NOT gates, we obtained results showing qualitatively similar behavior to the previous results presented in Refs. [24, 29] for a single RTN source. In particular, just as for a single noise source, in the presence of $1/f^\alpha$ noise we observed a transition in the optimal control pulse sequence from a constant pulse to a CORPSE-like sequence as the noise characteristic correlation time τ_c is increased.

This approach of coupled master equations indexed by noise states of the environment, together with an optimization technique for pulse design can be readily generalized to multiple qubits evolving in the presence of

$1/f^\alpha$ noise and other Markovian noise sources. Furthermore, it can be used to develop realistic pulse sequences for mitigation of nuclear spin and surface magnetic noise acting on donor spins implanted in silicon [11], as well as for suppression of background charge noise acting on superconducting qubits [4]. In future, we will study the implementation of multi-qubit gates, e.g., the controlled NOT gate, in noisy systems and the swapping of quantum information from a noisy qubit to long term quantum memory. We will also consider more realistic noise with $1/f^\alpha$ spectrum over many frequency decades.

Acknowledgments

This work was supported by the Academy of Finland, the National Security Agency (NSA) under MOD713106A and by the NSF ITR program under grant number EIA-0205641. M. M. and V. B. acknowledge the Finnish Cultural Foundation, M. M. the Väisälä foundation and Magnus Ehrnrooth Foundation for the financial support. We thank J. Clarke for insightful discussions.

-
- [1] L. Faoro and L. Viola, Phys. Rev. Lett. **92**, 117905 (2004).
 - [2] E. Paladino, L. Faoro, G. Falci, and R. Fazio, Phys. Rev. Lett. **88**, 228304 (2002).
 - [3] G. Falci, A. D'Arrigo, A. Mastellone, and E. Paladino, Phys. Rev. A **70**, 040101 (2004).
 - [4] O. Astafiev, Y. A. Pashkin, Y. Nakamura, T. Yamamoto, and J. S. Tsai, Phys. Rev. Lett. **96**, 137001 (2006).
 - [5] O. Astafiev, Y. A. Pashkin, Y. Nakamura, T. Yamamoto, and J. S. Tsai, Phys. Rev. Lett. **93**, 267007 (2004).
 - [6] F. C. Wellstood, C. Urbina, and J. Clarke, Apl. Phys. Lett. **85**, 5296 (2004).
 - [7] M. Mück, M. Korn, C. G. A. Muford, J. B. Kycia, and J. Clarke, Apl. Phys. Lett. **86**, 012610 (2005).
 - [8] T. M. Eiles, R. L. Kautz, and J. M. Martinis, Apl. Phys. Lett. **61**, 237 (1992).
 - [9] Y. Nakamura, Y. A. Pashkin, T. Yamamoto, and J. S. Tsai, Physica Scripta **102**, 155 (2002).
 - [10] R. de Sousa, unpublished, cond-mat/0610716 (2006).
 - [11] T. Schenkel, J. A. Liddle, A. Persaud, A. M. Tyryshkin, S. A. Lyon, R. de Sousa, K. B. Whaley, J. B. J. Shangkuan, and I. Chakarov, Apl. Phys. Lett. **8**, 11201 (2006).
 - [12] R. de Sousa *et al.*, unpublished (2007).
 - [13] Y. Nakamura, Y. A. Pashkin, T. Yamamoto, and J. S. Tsai, Phys. Rev. Lett. **88**, 047901 (2002).
 - [14] Y. M. Galperin, B. L. Altshuler, J. Bergli, and D. V. Shantsev, Phys. Rev. Lett. **96**, 097009 (2006).
 - [15] B. Savo, F. C. Wellstood, and J. Clarke, Appl. Phys. Lett. **50**, 1757 (1987).
 - [16] R. T. Wakai and D. J. V. Harlingen, Phys. Rev. Lett. **58**, 1687 (1987).
 - [17] T. Fujisawa and Y. Hirayama, Apl. Phys. Lett. **77**, 543 (2000).
 - [18] C. Kurdak, C.-J. Chen, D. C. Tsui, S. Parihar, S. Lyon, and G. W. Weimann, Phys. Rev. Lett. **56**, 9813 (1997).
 - [19] R. de Sousa, K. B. Whaley, F. K. Wilhelm, and J. von Delft, Phys. Rev. Lett. **95**, 247006 (2005).
 - [20] L. Viola and S. Lloyd, Phys. Rev. A **58**, 2733 (1998).
 - [21] L. Viola, S. Lloyd, and E. Knill, Phys. Rev. Lett. **83**, 4888 (1999).
 - [22] A. G. Kofman and G. Kurizki, Phys. Rev. Lett. **87**, 270405 (2001).
 - [23] A. G. Kofman and G. Kurizki, Phys. Rev. Lett. **93**, 130406 (2004).
 - [24] M. Möttönen, R. d. Sousa, J. Zhang, and K. B. Whaley, Phys. Rev. A **73**, 022332 (2006).
 - [25] M. B. Weissman, Rev. Mod. Phys. **60**, 537 (1988).
 - [26] E. Paladino, L. Faoro, G. Falci, and R. Fazio, Phys. Rev. Lett. **88**, 228304 (2002).
 - [27] B. Kaulakys, V. Gontis, and M. Alaburda, Phys. Rev. E **71**, 051105 (2005).
 - [28] Y. M. Galperin, B. L. Altshuler, J. Bergli, and D. V. Shantsev, Phys. Rev. Lett. **96**, 097009 (2006).
 - [29] O.-P. Saira, V. Bergholm, T. Ojanen, and M. Möttönen, Phys. Rev. A **75**, 012308 (2007).
 - [30] M. J. Kirton and M. J. Uren, Advances in Physics **38** (1989).
 - [31] N. Khaneja, T. Reiss, C. Kehlet, T. Schulte-Herbrüggen, and S. J. Glaser, J. Mag. Res. **172**, 296 (2005).
 - [32] H. K. Cummins and J. A. Jones, New J. Phys. **2**, 1 (2000).
 - [33] H. K. Cummins, G. Llewellyn, and J. A. Jones, Phys. Rev. A **67**, 042308 (2003).
 - [34] S. Meiboom and D. Gill, Rev. Sci. Instr. **29**, 688 (1958).
 - [35] J. L. Hennessy and D. A. Patterson, *Computer Architecture: A Quantitative Approach* (Morgan Kaufmann, 2006).